

Provided for non-commercial research and education use.
Not for reproduction, distribution or commercial use.



This article appeared in a journal published by Elsevier. The attached copy is furnished to the author for internal non-commercial research and education use, including for instruction at the authors institution and sharing with colleagues.

Other uses, including reproduction and distribution, or selling or licensing copies, or posting to personal, institutional or third party websites are prohibited.

In most cases authors are permitted to post their version of the article (e.g. in Word or Tex form) to their personal website or institutional repository. Authors requiring further information regarding Elsevier's archiving and manuscript policies are encouraged to visit:

<http://www.elsevier.com/copyright>



Coarsening of extracellularly biosynthesized cadmium crystal particles induced by thioacetamide in solution

Gui-Qiu Chen^{*}, Zheng-Jun Zou, Guang-Ming Zeng^{*}, Ming Yan, Jia-Qi Fan, An-Wei Chen, Fan Yang, Wen-Juan Zhang, Liang Wang

College of Environmental Science and Engineering, Hunan University, Changsha 410082, PR China

Key Laboratory of Environmental Biology and Pollution Control (Hunan University), Ministry of Education, Changsha 410082, PR China

ARTICLE INFO

Article history:

Received 27 November 2010

Received in revised form 31 March 2011

Accepted 31 March 2011

Available online 13 April 2011

Keywords:

White rot fungus

Crystal particle

Extracellular

Cadmium

Coarsening

ABSTRACT

A novel coarsening route for extracellularly biosynthesized cadmium nanocrystals was investigated for the first time. In this process, the white rot fungus *Coriolus versicolor* was employed to take up cadmium ions and synthesize extracellular cadmium crystal particles. The coarsening of the particles was induced by thioacetamide under certain conditions. Scanning electron microscopy showed that the formed cadmium crystal particles were coarsened from about 100 nm to 2–3 μm . The corresponding energy-dispersive X-ray spectra confirmed the presence of proteins in the particles. The maximum removal efficiency of Cd(II) increased from 17% to 87%, and the corresponding sorption capacity of biomass increased from 4 to 24 mg g^{-1} with the completion of the coarsening process. The properties of the coarsened particles were also examined using X-ray diffraction (XRD) and transmission electron microscopy (TEM). XRD analysis of fungal mycelial pellets embedded with the coarsened particles confirmed the formation of cubic crystalline cadmium sulfide particles. The TEM results suggest that the coarsened particles were composed of clusters of several smaller particles. The changes in the functional groups on the biomass surface were studied through Fourier transform infrared spectroscopy. Based on the results above, a possible mechanism for the formation and coarsening of cadmium crystal particle is also discussed.

© 2011 Elsevier Ltd. All rights reserved.

1. Introduction

Recent investigations by various research groups have shown that metallic crystals can be extracellularly biosynthesized by many microorganisms under suitable conditions in toxic metal-contaminated water. Extracellular biosynthesis has been recognized as a defense mechanism against toxicity of microbes. For example, white rot fungi (Jarosz-Wilkolazka and Gadd, 2003; Huang et al., 2008), brown rot fungi (Jarosz-Wilkolazka and Gadd, 2003), and sulfate-reducing bacteria (Suzuki et al., 2002) have been found to have the capacity to sequester heavy metals into metal nanocrystals under certain conditions in response to heavy metal stress.

Commonly, these formed crystal particles are in the nanometer range, which make them still highly mobile and have the ability to redissolve if the conditions change (Moreau et al., 2009). These properties of nanocrystals may lead to recontamination of the

water and will increase the separation cost of the wastewater treatment process. An earlier study has reported that coarsening could restrict nanoparticle transport by inducing settling (Bradford et al., 2002), driving crystal growth, and result in decreased solubility (Moreau et al., 2009). Therefore, to decrease the solubility and mobility of metal nanocrystals in the solution and to lower the separation cost during wastewater treatment, there is an imperative need for methods that facilitate nanocrystal coarsening.

In previous studies (Chen et al., 2005, 2006, 2008), we found that the quantity of heavy metals taken up by *Lentinula edodes* far exceeds the amount estimated from the sorption sites of the microorganism. Extracellular biosynthesis of metal crystal particles has been considered a contributor to this phenomenon. To date, however, few studies have been conducted to investigate the mechanisms for nanocrystal formation and coarsening, which may enhance the removal capacity of the biomass and decrease the biological treatment cost of toxic metals. Thus, nanocrystal formation and coarsening mechanisms is discussed in the current study.

In the present study, *C. versicolor* was used to biosynthesize cadmium crystal particles and nanocrystal coarsening was facilitated by the addition of thioacetamide (TAA). We report here our findings that the cadmium nanocrystals could be extracellularly bio-

^{*} Corresponding authors at: College of Environmental Science and Engineering, Hunan University, Changsha 410082, PR China. Tel.: +86 731 88822829; fax: +86 731 88823701.

E-mail addresses: gqchen@hnu.cn (G.-Q. Chen), zgming@hnu.cn (G.-M. Zeng).

synthesized using *C. versicolor* and their coarsening could be induced by TAA under certain conditions.

To the best of our knowledge, this is the first report showing TAA-induced coarsening of extracellularly biosynthesized cadmium nanocrystals. The possible underlying mechanisms are also discussed. Although metal nanocrystals have been biosynthesized using fungi such as *Fusarium oxysporum* (Ahmad et al., 2002), *Verticillium sp.* (Sastry et al., 2003), and *Phanerochaete chrysosporium* (Sanghi and Verma, 2009b), the coarsening of the nanoparticles induced by additional TAA has never been mentioned. Furthermore, the sorption performance investigated in the current study indicates that the maximum removal efficiency of Cd(II) is significantly enhanced with the completion of the coarsening process, which reveals that this process possesses tremendous potential for biological treatment of toxic metals.

2. Materials and methods

2.1. Fungus culture

The white rot fungal strain *C. versicolor* (ACCC 51171) was obtained from the Institute of Agricultural Resources and Regional Planning, Chinese Academy Agricultural Science. The strain was maintained at 4 °C on potato dextrose agar slants. The fungus was cultivated in liquid medium using shake flask method. Erlenmeyer flasks (250 mL) were used for growing the fungal mycelia. The flask contained 100 mL of the growth medium. The medium was composed of the following (g L⁻¹ of distilled water): dextrose anhydrous, 10; ammonium tartrate, 1; KH₂PO₄, 2; MgSO₄·7H₂O, 0.5; CaCl₂·2H₂O, 0.1; vitamin B1, 0.001; and 7 mL of trace element mixed liquor. The trace element mixed liquor contained the following (g L⁻¹ of distilled water): aminoacetic acid, 0.5; MgSO₄·7H₂O, 3; NaCl, 1; FeSO₄·H₂O, 0.1; CoSO₄, 0.1; CaCl₂·2H₂O, 0.1; ZnSO₄·7H₂O, 0.1; CuSO₄·5H₂O, 0.01; KAl(SO₄)₂·12H₂O, 0.01; Na₂MoO₄·12H₂O, 0.01; MnSO₄·H₂O, 0.5; and H₃BO₃, 0.01.

The flasks were inoculated with three agar plugs (diameter, 3 mm) excised from a fungal colony growing on a dextrose potato extract plate and cultivated at 30 °C under shaking (200 rpm) for 2–3 d to prepare inocula. Then, 2 mL of the inocula was transferred to the autoclaved media under sterilized conditions and allowed to grow for 4–5 d in a shaker (150 rpm) at 25–30 °C. The mycelium pellets spontaneously formed in the media. The media were autoclaved at 105 °C for 30 min and cooled to room temperature before use. The pH after autoclaving was 5.6.

2.2. Preparation of solutions

All reagents used were of analytical grade and purchased from Tianjin Pharmaceutical Co., China. The 1 g L⁻¹ of stock Cd(II) solution was prepared by dissolving 2.775 g of Cd(NO₃)₂·4(H₂O) in 1 L of deionized water. The 0.668 g L⁻¹ of fresh TAA solution was prepared by dissolving 0.668 g C₂H₅NS (purity ≥ 99.0%) in 1 L of deionized water.

2.3. Adsorption experiment and size control

After the mycelium pellets formed, two types of experiments were conducted. Biosorption of Cd(II) by *C. versicolor* was first investigated, followed by coarsening of cadmium crystal particles. In the first group of experiments, 1 mL of stock Cd(II) solution (1 g L⁻¹) was added to the media with an initial Cd(II) concentration of about 10 mg L⁻¹. In the second group of experiments, 1 mL of fresh TAA (0.668 g L⁻¹) was added to the media after Cd(II) was added for 24 h when adsorption equilibrium reached. The time of adsorption equilibrium was obtained from the result of the first

group of experiments. For both groups of experiments, the concentrations of Cd(II) and dissolved protein at given time intervals (0–60 h) were determined. The concentration of Cd(II) was determined using a Flame Atomic Absorption Spectrometer (PerkinElmer AA700, USA). The content of the dissolved protein was determined via the Coomassie Brilliant Blue method using UV-Vis (UV754N, Shanghai, China) at 595 nm.

2.4. Scanning electron microscopy (SEM) coupled with energy-dispersive X-ray (EDX) analysis

The mycelium pellets were harvested through filtering after 60 h incubation, washed with distilled water, and then dried under –40 °C in a freezer dryer (FD-1, Boyikang, Beijing, China). The samples of the dry mycelium pellets (native, treated with cadmium ions, treated with cadmium ions and TAA) were measured on an SEM (FEI QUANTA-200, Holland FEI Company, Holland) equipped with an EDX attachment. The micrographs were taken and their corresponding EDX spectra were recorded by focusing on selected points of particles.

2.5. TEM analysis

The mycelium pellets (treated with cadmium ions and TAA) were harvested after 60 h incubation and washed with distilled water. The cadmium crystal particles still attached to the mycelia were dispersed in water by ultrasonication. For TEM, a drop of aqueous solution containing cadmium crystal particles was placed on a carbon-coated copper grid and was air-dried. Transmission electron micrographs were obtained using a TEM (H-800, Hitachi, Japan).

2.6. XRD and Fourier transform infrared (FTIR) analysis

The freeze-dried mycelium pellets (treated with cadmium ions and TAA) embedded with cadmium crystal particles were powdered and used for XRD analysis. The pattern was recorded using an automatic X-ray diffractometer (D8-Advance, Bruker Company, German). For FTIR, the freeze-dried mycelium pellets (native, treated with cadmium ions, and treated with cadmium ions and TAA) were powdered. Their IR spectra were recorded on an IR spectrophotometer (WQF-410, Beijing, China) making KBr pellets in reflectance mode.

3. Results and discussion

3.1. SEM-EDX analysis

To facilitate the coarsening of cadmium crystal particles, a given amount of TAA was added into the media in which cadmium ions had been absorbed for 24 h, when the adsorption equilibrium reached (estimated from Fig. 1a). The SEM technique could describe the surface characteristics of the fungus, so it was employed to observe the changes in particle size. The SEM images of the native fungus, the cadmium-treated fungus, and the cadmium and TAA-treated fungus are presented in Fig. 2. In Fig. 2a, the surface of the native fungus was smooth and clear, without any adsorbed particles. As shown in Fig. 2b and c, many light dots (cadmium-binding particles) were highly dispersed on the mycelial surface. The outline of the mycelium showed some deformations from reacting with cadmium ions, similar to that obtained from our unpublished data on *P. chrysosporium* reacting with Cd(II). From the images, the average diameter of the cadmium-binding particles was about 100 nm. Compared with Fig. 2b and c, Fig. 2d and e illustrate that many 2–3 μm cadmium-binding particles were obtained

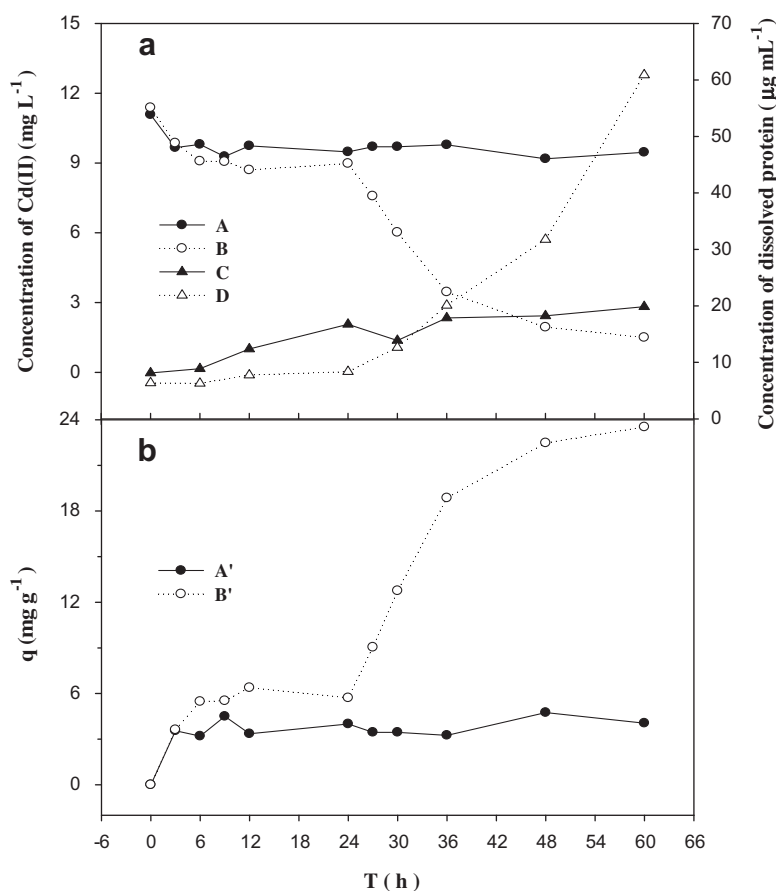


Fig. 1. (a). Time course of cadmium uptake (A and B) and dissolved protein secretion (C and D): A and C (no TAA added), B and D (TAA added); (b). The corresponding sorption capacity of the biomass: A' (no TAA added), B' (TAA added), q was the amount of Cd(II) adsorbed by biomass (mg g^{-1}).

after TAA was added. These particles were cubic and uniform in size. These results indicated that the cadmium-binding particles were successfully induced to coarsen by the addition of TAA. This is a great advantage in wastewater treatment because coarsened particles are easier to separate using common filtration techniques than particles in the nanometer range. Consequently, separation cost is reduced. This coarsening process also decreases the solubility and mobility of metal nanocrystals in the solution, thereby reducing the risk of water recontamination. The possible mechanism for the coarsening of the particles is illustrated in Section 3.5.

EDX is a reliable method for determining the elemental composition of particles. The EDX data of a selected point from the cubic particles (red point in Fig. 2e) shown in Fig. 2f revealed the presence of carbon, nitrogen, oxygen, phosphorus, sulfur, and cadmium. The cadmium peak demonstrates the binding of cadmium ions onto the surface of the biomass. Nitrogen signals were also observed in the EDX spectra, specifically indicating the presence of amino acids or even proteins. These results were in agreement with phenomena observed in earlier studies (Gole et al., 2001; Lin et al., 2005; Vigneshwaran et al., 2006), which confirmed that proteins play an important role in the formation and stabilization of metal nanoparticles. The peaks for carbon, oxygen, and phosphorus were characteristics of the composition of many organic substances in the cell wall of the biomass.

3.2. Removal of cadmium ions

To understand the changes in Cd(II) removal efficiency in the two experiments (with or without TAA), the Cd(II) concentration in the media was determined at given intervals (0–60 h). The re-

sults are shown in Fig. 1a. The removal efficiency of the cadmium ions improved after TAA was added. The maximum was 87%, compared with 17% for the control. The corresponding sorption capacity of the biomass was 24 mg g^{-1} compared with 4 mg g^{-1} (Fig. 1b). These findings demonstrate that the Cd(II) removal capacity of the biomass increases with the increase of particle size. A contributing factor to this may be the variation in the existing form of cadmium ion, from the chelated form to CdS, which alters the accumulation of cadmium ions. Although this phenomenon has not been observed among fungi, similar results have been observed in *Phaeodactylum tricornutum* by Scarano and Morelli (2003).

Dissolved protein content was also determined at the given intervals. The data are presented in Fig. 1a. As shown in the figure, dissolved protein content increased in various ways in the two experiments. In the control experiment, it slowly increased, with the maximum reaching 20 µg L^{-1} at 60 h. In contrast, in the TAA treatment, it rapidly increased after the addition of TAA, and the maximum was 61 µg L^{-1} at 60 h. The fungal secretion of proteins may be a defense mechanism in response to stimulation by cadmium ions. Oxygenous or nitrogenous functional groups, such as carboxyl, amino, and peptide bonds, in the proteins of microbial cell walls have been suggested to be responsible for the binding of metal ions in microorganisms (Lin et al., 2005). Özcan et al. (2007) proved that *P. chrysosporium* secreted some proteins, such as glucose-6-phosphate isomerase, ribosomal protein S7, and ribosomal protein S21e, in response to heavy metal stress. Moreover, proteins have been found to play an important role in the stabilization of metal nanoparticles (Vigneshwaran et al., 2006) and in the aggregation of small particles (Moreau et al., 2009). Thus, the secretion of protein by the fungus in the experiment provided

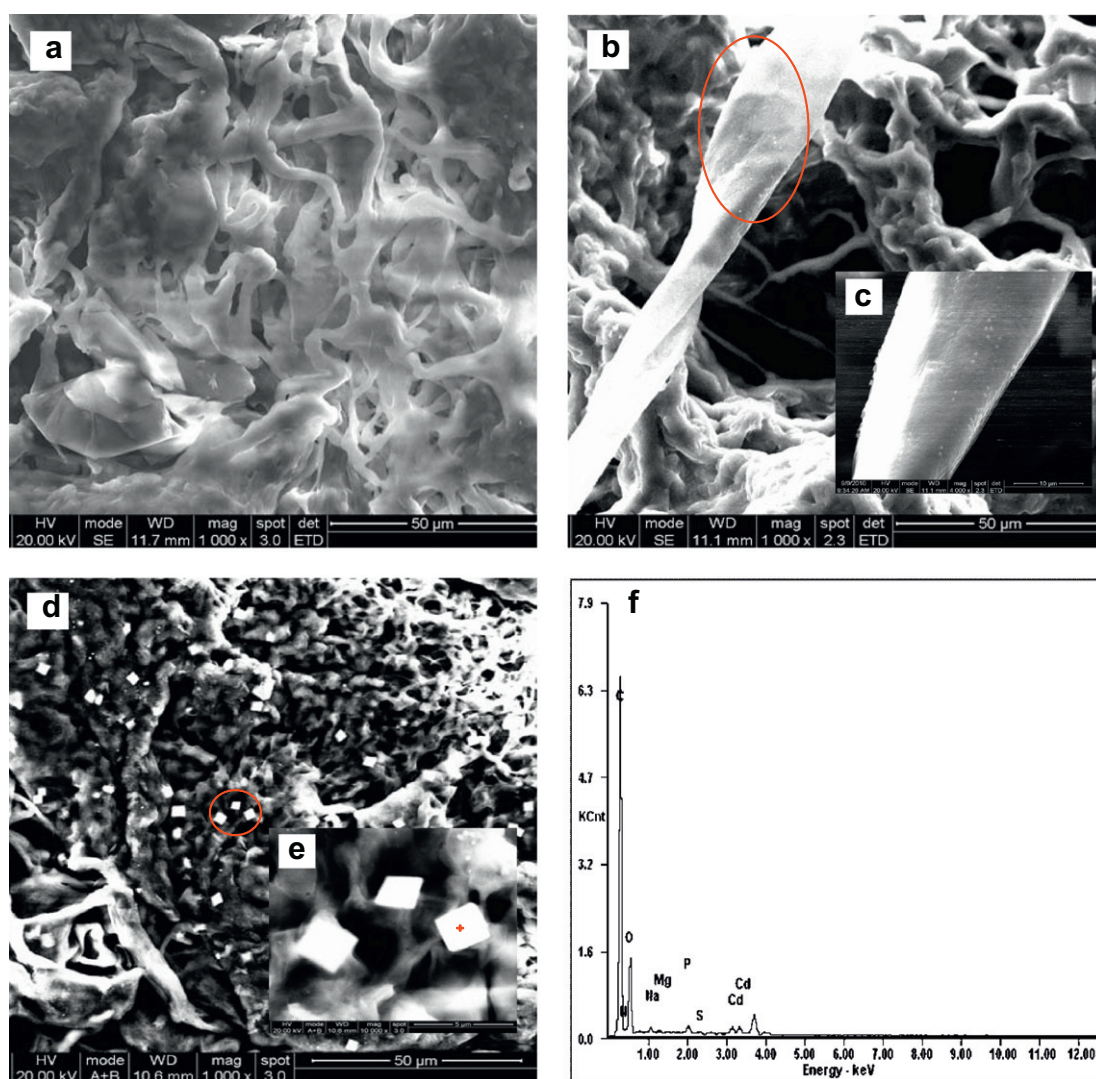


Fig. 2. SEM-EDX micrograph of mycelium pellets: (a), native; (b) and (c), treated with Cd(II) (c was the magnification of selected area in b with scale bar 10 µm); (d) and (e), treated with Cd(II) and then TAA (e was the magnification of selected area in d with scale bar 5 µm); (f), EDX graph of selected point (the red point in e). (For color interpretation in this figure legend the reader is referred to see the web version of this article.)

materials for cadmium ion removal, stabilization of cadmium crystal particles, and even aggregation of small particles.

3.3. TEM and XRD analyses

Determining the exact nature of the cadmium crystal particles, which can be deduced by TEM and XRD analyses, is important. For TEM, mycelial pellets challenged with Cd(II) and then TAA were examined. The TEM image (Fig. 3) shows that the cadmium crystal particles were not uniform in size and shape. Some aggregation of the particles could also be observed. This could be related to the preparation technique that deposited the particles onto the copper grid. The average size of the particles estimated from the image was in the 20–40 nm range, which does not agree with the size estimated by SEM (Fig. 2d and e). This phenomenon shows that the cubic particles seen under SEM are actually clusters of several small particles with different sizes. As discussed, amino acids or proteins might play a role in this aggregation process.

Further studies were carried out using XRD, an effective method for investigating the microstructure of crystalline or amorphous materials, to confirm the crystalline nature of the coarsened particles. The XRD pattern obtained is shown in Fig. 4. The XRD pattern

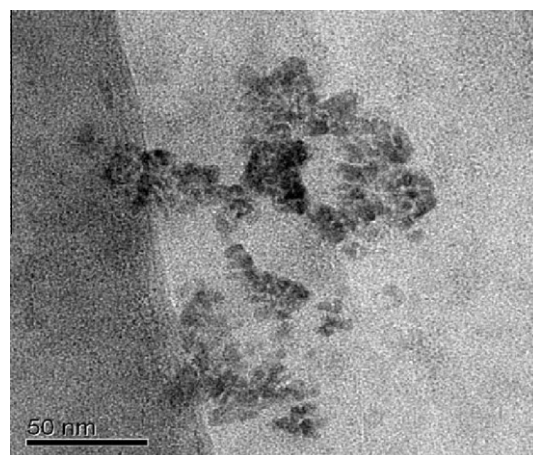


Fig. 3. Transmission electron micrographs of cadmium crystal particles with scale bar 50 nm.

exhibits three intense peaks at 2θ values of 26.50, 43.96, and 52.13°, which could be indexed to the (1 1 1), (2 2 0), and (3 1 1)

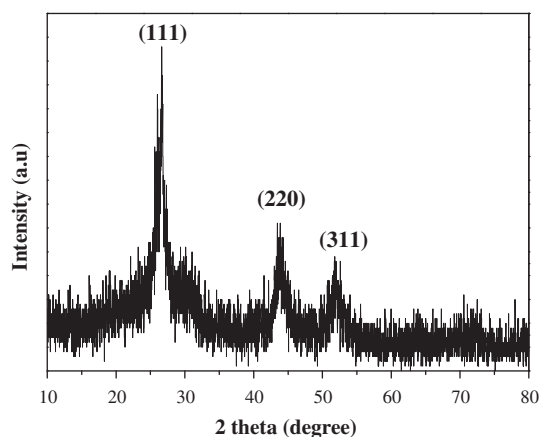


Fig. 4. XRD pattern of fungus sample challenged with Cd(II) and TAA.

facets of the cubic phase CdS, respectively (JCPDS Powder Diffraction File no. 10-454). These three intense peaks agree with the Bragg's reflection of CdS nanocrystals reported in the literature (Rodríguez et al., 2008). The broadened peaks indicate that the sizes of the particles are in the nanometer range (Bai et al., 2009), in line with the size estimated from the TEM image. The shoulder in the (1 1 1) diffraction peak may have resulted from the X-ray irradiation on the sample (Wang et al., 2003). Moreover, two small insignificant impurity peaks were observed at 64° and 68°, which may be attributed to other organic substances of the fungal mycelia. The results indicate that the square particles (Fig. 2d and e) formed on the fungal surface were cubic phase CdS nanocrystals.

3.4. FTIR analysis

To study cadmium crystal particle formation and coarsening mechanism in the system, the FTIR spectra of the native fungi, the Cd(II)-treated fungi, and the fungi treated with Cd(II) and TAA were determined. The FTIR spectrum displays a number of absorption peaks due to the several functional groups present in the fungal cell walls (Fig. 5).

The strong broad IR absorption band of the native fungus at around 3365 cm^{-1} is characteristic of the O–H stretching vibration in the carboxyl group. In the 3500–3300 cm^{-1} region, the N–H

stretching vibration bands of the fungal mass may overlap with the strong and large band of the carboxyl group (Choi and Yun, 2006). The peaks observed at 2927 and 2858 cm^{-1} could be assigned to the anti-symmetric and symmetric vibrations of the CH_2 groups of the hydrocarbons present in fungal protein. The bands at around 2560 and 671 cm^{-1} were due to –SH and C–S stretching, respectively, and these are characteristic of sulfur-bearing protein residues such as cysteine and methionine. The spectrum also displays absorption peaks at 1660 and 1545 cm^{-1} , corresponding to C=O and N–H stretching, which correspond to amide I and II, characteristic of polypeptides or proteins (Moreau et al., 2009). The amide II band at 1545 cm^{-1} also represents the asymmetric stretching vibration of COO in the carboxylates overlapping with the C–N stretching of O=C–N–H (Sanghi et al., 2009). The most complex amide III bands were also seen between 1300 and 1200 cm^{-1} . The presence of carbonyl groups is evident from the characteristic absorption peaks around 3365 cm^{-1} , representing O–H stretching, and around 1660 and 1240 cm^{-1} , representing C=O stretching. The C–N stretching of aliphatic amines is evident from the peak at 1043 cm^{-1} (1090–1020 cm^{-1}). In addition, the spectrum also shows the peculiar absorption band between 600 and 550 cm^{-1} due to C–N–C scissoring, which is only found in the polypeptide spectra (Sanghi et al., 2009).

Some changes could be observed in the spectrum by comparing the initial state of the biomass with that after treatment with Cd(II) or with both Cd(II) and TAA. The main changes are presented in Table 1. The characteristic peaks of the stretching vibrations of –NH and –OH (COOH) shifted to a low wave number of about 4 cm^{-1} for the Cd(II)-treated fungi and 6 cm^{-1} for the fungi treated with Cd(II) and TAA. The intensity of the peaks also weakened (Fig. 5), which indicates that the nitrogen and oxygen atoms were the binding sites for Cd(II) on the fungi during the reaction. The most differences were that the peak of stretching vibrations of –SH disappeared after the two treatments and the peak for the stretching vibrations of C–S shifted to higher wave numbers by approximately 17 and 8 cm^{-1} , respectively. The reason for this may be the replacement of the H atom of –SH by Cd, forming the Cd–S–R complex on the grown CdS crystal surface (Tang et al., 2005; Sanghi and Verma, 2009a). The slight blue shift in the amide I band from 1660 to 1658 cm^{-1} for the Cd-treated fungi and to 1656 cm^{-1} for the fungi treated with Cd and TAA indicates that some interactions between Cd(II) and C=O occurred (Yang et al., 2006). The shifts in wavelength and the variation in transmittances of the amide II band and the C–N absorption peak are also shown

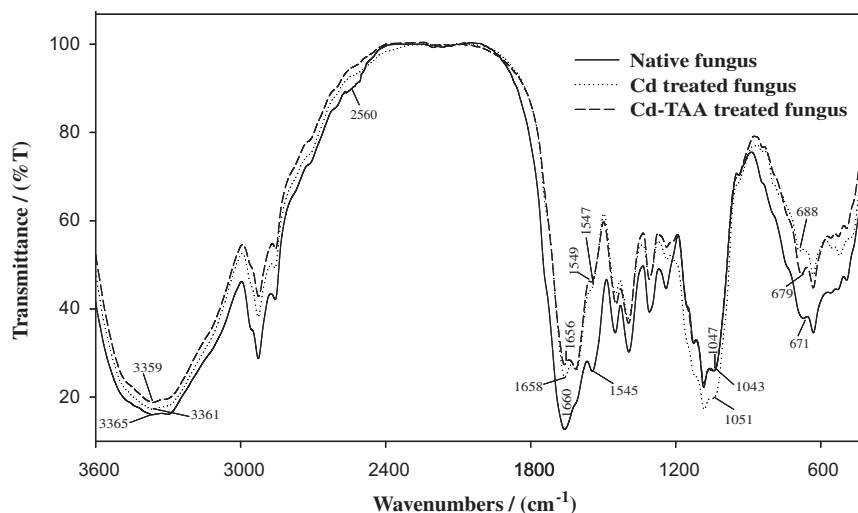


Fig. 5. FTIR spectra of native fungus, Cd(II) treated fungus and Cd-TAA treated fungus.

Table 1

The main IR peaks of native fungus, Cd(II) treated fungus and Cd(II)-TAA treated fungus.

Assignment (cm ⁻¹)	-OH	-SH	Amide I	Amide II	-CN	C-S
Native fungus	3365	2560	1660	1545	1043	671
Cd-fungus	3361	–	1658	1547	1051	688
Cd-TAA-fungus	3359	–	1656	1549	1047	679

in Table 1 and Fig. 5. Based on the shift in the amide I and II bands coupled with the variations in the transmittances, the conformation of the proteins may have been affected because of the reaction with cadmium ions or binding with the cadmium sulfide crystal particles, as described by Sanghi and Verma (2009b).

The carbonyl group of amino acid residues and peptides has a strong ability to bind metals (Gole et al., 2001; Vigneshwaran et al., 2006), and proteins can bind to nanoparticles either through free amine groups (not reacting with carboxyl groups in the formation of peptide chain) or cysteine residues, and via the electrostatic attraction of the negatively charged carboxylate groups in the enzymes present in the cell wall of mycelia (Gole et al., 2001; Sanghi and Verma, 2009b). The sulfhydryl group present in cysteine and mercapto-compounds particularly exhibit strong specific binding to the surfaces of sulfide minerals and nanoparticles (Moreau et al., 2009). Based on the analyses, the proteins secreted by the fungus could possibly form a coat that covers the metal nanoparticles to prevent their agglomeration and aid in their stabilization in the medium.

3.5. Possible mechanism

Based on the results and discussion above, a possible formation mechanism for the cubic CdS crystal particles (Fig. 2d and e) is proposed. Initially, the cadmium ions are captured by the biomolecules secreted by the fungi through chelation via the carboxyl, amino, and thiol groups on the fungal cell wall or released into the solution. The extracellular chelating compounds could link together and form Cd-binding particles (Figs. 2b and c) on the fungal cell wall. When TAA is introduced, S(II) is slowly released into the solution through hydrolysis. The S(II) may then destroy complexes, such as Cd–S–R, and combine with Cd(II) to form the CdS nuclei due to their stronger interactions. The residual Cd–S–R complexes may covalently bind to the CdS core (Tang et al., 2005) and form passivation layers, thereby preventing the growth of CdS nanocrystals. At the same time, other biomolecules containing carboxylic acid and carboxylate also have the capacity to assemble onto the surface of CdS nanocrystals, and in turn are responsible for capping the CdS nanocrystals via hydrogen bonding and electrostatic interaction (Sanghi and Verma, 2009a).

However, monodispersed CdS nanocrystals could not be obtained because water, hydroxyl group (Yan et al., 2004), and amino acids (Moreau et al., 2009) could impel the agglomeration of CdS nanocrystals. These associations, coupled with the interactions between CdS nuclei may be the driving force for the formation of cubic micro-particles (Figs. 2d and e). The formation of special cubic structures may be due to different growth rates of nanocrystals in all directions, because if the growth rate in all directions is slow, the shape of the CdS crystals will be spherical due to minimum surface energy effect (Maleki et al., 2008). The parameters affecting crystal growth are complicated and include the internal structure of a given crystal, capping molecule, temperature, and mass transport. However, the key parameter is the internal structure of the given crystal (Zhang et al., 2007). Therefore, further investigations are needed to derive the exact mechanism.

4. Conclusions

This study has demonstrated a novel process for the extracellular induction of cadmium nanocrystal coarsening using additional TAA. When the coarsening was completed, cadmium ion removal efficiency greatly improved from 17% to 87% (corresponding to the sorption capacity of biomass from 4 to 24 mg g⁻¹). The results of SEM-EDX indicate that particle coarsening and the presence of proteins in the particles. TEM analysis suggests the coarsened particles seen under SEM (Fig. 2d and e) were actually composed of clusters of several different-sized particles. Characterization of the coarsened particles by XRD techniques confirmed the formation of cubic crystalline cadmium sulfide particles. In addition, FTIR analysis revealed the important role of proteins in the formation and coarsening of cadmium nanocrystals. The mechanisms discussed in this article may be of great use in conducting biological remediation of toxic metals and improving their efficiency in the future. Another potential benefit of the process described in the current study is that it will provide practical and theoretical reference values for the extracellular biosynthesis and controlling the size of metal nanoparticles.

Acknowledgments

This study was financially supported by the National Natural Science Foundation of China (50908078, 50978088, 51039001), Xiangjiang Water Environmental Pollution Control Project subjected to the National Key Science and Technology Project for Water Environmental Pollution Control (2009ZX07212-001-02 and 2009ZX07212-001-06), the Program for Changjiang Scholars and Innovative Research Team in University (IRT0719), the National Basic Research Program (973 Program) (2005CB724203), the Hunan Key Scientific Research Project (2009FJ1010), and the Hunan Provincial Natural Science Foundation of China (10JJ7005).

References

- Ahmad, A., Mukherjee, P., Mandal, D., Senapati, S., Khan, M.I., Kumar, R., Sastry, M., 2002. Enzyme mediated extracellular synthesis of CdS nanoparticles by the fungus, *Fusarium oxysporum*. *J. Am. Chem. Soc.* 124, 12108–12109.
- Bai, H.J., Zhang, Z.M., Guo, Y., Jia, W.L., 2009. Biological synthesis of size-controlled cadmium sulfide nanoparticles using immobilized *Rhodobacter sphaeroides*. *Nanoscale Res. Lett.* 4, 717–723.
- Bradford, S.A., Yates, S.R., Bettehar, M., Simunek, J., 2002. Physical factors affecting the transport and fate of colloids in saturated porous media. *Water Resour. Res.* 38, 1327.
- Chen, G.Q., Zeng, G.M., Tang, L., Du, C.Y., Jiang, X.Y., Huang, G.H., Liu, H.L., Shen, G.L., 2008. Cadmium removal from simulated wastewater to biomass byproduct of *Lentinus edodes*. *Bioresour. Technol.* 99, 7034–7040.
- Chen, G.Q., Zeng, G.M., Tu, X., Huang, G.H., Chen, Y.N., 2005. A novel biosorbent: characterization of the spent mushroom compost and its application for removal of heavy metals. *J. Environ. Sci.* 17, 756–760.
- Chen, G.Q., Zeng, G.M., Tu, X., Niu, C.G., Huang, G.H., Jiang, W., 2006. Application of a by-product of *Lentinus edodes* to the bioremediation of chromate contaminated water. *J. Hazard. Mater.* B135, 249–255.
- Choi, S.B., Yun, Y.S., 2006. Biosorption of cadmium by various types of dried sludge: an equilibrium study and investigation of mechanisms. *J. Hazard. Mater.* B138, 378–383.
- Gole, A., Dash, C., Ramakrishnan, V., Sainkar, S.R., Mandale, A.B., Rao, M., Sastry, M., 2001. Pepsin-gold colloid conjugates: preparation, characterization, and enzymatic. *Langmuir* 17, 1674–1679.
- Huang, D.L., Zeng, G.M., Feng, C.L., Hu, S., Jiang, X.Y., Tang, L., Su, F.F., Zhang, Y., Zeng, W., Liu, H.L., 2008. Degradation of lead-contaminated lignocellulosic waste by *Phanerochaete chrysosporium* and the reduction of lead toxicity. *Environ. Sci. Technol.* 42, 4946–4951.
- Jarosz-Wilkolazka, A., Gadd, G.M., 2003. Oxalate production by wood-rotting fungi growing in toxic metal-amended medium. *Chemosphere* 52, 541–547.
- Lin, Z.Y., Zhou, C.H., Wu, J.M., Zhou, J.Z., Wang, L., 2005. A further insight into the mechanism of Ag⁺ biosorption by *Lactobacillus sp.* strain A09. *Spectrochim. Acta A* 61, 1195–1200.
- Maleki, M., Mirdamadi, S., Ghasemzadeh, R., Ghamsari, M.S., 2008. Preparation and characterization of cadmium sulfide nanorods by novel solvothermal method. *Mater. Lett.* 62, 1993–1995.

- Moreau, J.W., Weber, P.K., Martin, M.C., Gilbert, B., Hutcheon, I.D., Banfield, J.F., 2009. Extracellular proteins limit the dispersal of biogenic nanoparticles. *Science* 316, 1600–1603.
- Özcan, S., Yildirim, V., Kaya, L., Albrecht, D., Becher, D., Hecker, M., Özcengiz, G., 2007. *Phanerochaete chrysosporium* soluble proteome as a prelude for the analysis of heavy metal stress response. *Proteomics* 7, 1249–1260.
- Rodríguez, P., Muñoz-Aguirre, N., Martínez, E.S., Gonzalez, G., Zelaya, O., Mendoza, J., 2008. Formation of CdS nanoparticles using starch as capping agent. *Appl. Surf. Sci.* 255, 740–742.
- Sanghi, R., Sankararamakrishnan, N., Dave, B.C., 2009. Fungal bioremediation of chromates: conformational changes of biomass during sequestration, binding, and reduction of hexavalent chromium ions. *J. Hazard. Mater.* 169, 1074–1080.
- Sanghi, R., Verma, P., 2009a. A facile green extracellular biosynthesis of CdS nanoparticles by immobilized fungus. *Chem. Eng. J.* 155, 886–891.
- Sanghi, R., Verma, P., 2009b. Biomimetic synthesis and characterisation of protein capped silver nanoparticles. *Bioresour. Technol.* 100, 501–504.
- Sastry, M., Ahmad, A., Khan, M.I., Kumar, R., 2003. Biosynthesis of metal nanoparticles using fungi and actinomycete. *Curr. Sci.* 85, 162–170.
- Scarano, G., Morelli, E., 2003. Properties of phytochelatin-coated CdS nanocrystallites formed in a marine phytoplanktonic alga (*Phaeodactylum tricorutum*, Bohlin) in response to Cd. *Plant Sci.* 165, 803–810.
- Suzuki, Y., Kelly, S.D., Kemner, K.M., Banfield, J.F., 2002. Radionuclide contamination: nanometer-size products of uranium bioreduction. *Nature* 419, 134.
- Tang, H.X., Yan, M., Zhang, H., Xia, M.Z., Yang, D.R., 2005. Preparation and characterization of water-soluble CdS nanocrystals by surface modification of ethylene diamine. *Mater. Lett.* 59, 1024–1027.
- Vigneshwaran, N., Kathe, A.A., Varadarajan, P.V., Nachane, R.P., Balasubramanya, R.H., 2006. Biomimetics of silver nanoparticles by white rot fungus, *Phanerochaete chrysosporium*. *Colloids Surf., B* 53, 55–59.
- Wang, W.Z., Liu, Z.H., Zheng, C.L., Xu, C.K., Liu, Y.K., Wang, G.H., 2003. Synthesis of CdS nanoparticles by a novel and simple one-step, solid-state reaction in the presence of a nonionic surfactant. *Mater. Lett.* 57, 2755–2760.
- Yan, B., Chen, D.R., Jiao, X.L., 2004. Synthesis, characterization and fluorescence property of CdS/P (N-iPAAm) nanocomposites. *Mater. Res. Bull.* 39, 1655–1662.
- Yang, L., Shen, Q.M., Zhou, J.G., Jiang, K., 2006. Biomimetic synthesis of CdS nanocrystals in aqueous solution of pepsin. *Mater. Chem. Phys.* 98, 125–130.
- Zhang, H., Yang, D.R., Ma, X.Y., 2007. Synthesis of flower-like CdS nanostructures by organic-free hydrothermal process and their optical properties. *Mater. Lett.* 61, 3507–3510.